Midrange Estimation for Sensor Fusion

Arash Komaee

***Abstract*— A nonlinear estimation technique is proposed to combine a precise but inaccurate sensor with an accurate but imprecise one in such a manner that their fusion enables both precise and accurate measurement of a physical quantity. This estimation technique solely relies on certain bounds on the measurement noise, rather than a detailed statistical description of the noise and the measured quantity. The estimation strategy is to estimate the slowly-varying offset of the inaccurate sensor based on a dynamic model for its temporal evolution, and the observations of the imprecise sensor. This measurement offset is estimated by recursively generating some tight upper and lower bounds for it, and then, taking the midpoint of these bounds as its *midrange estimation*. This estimation technique is verified effective both analytically and by Monte Carlo simulations.**

I. Introduction

This paper presents a nonlinear estimation technique for fusion of a precise but inaccurate sensor with an accurate but imprecise counterpart in order to enhance both precision and accuracy of measurement. The first sensor is precise in the sense that its reading consistently stays the same in repeated measurements of a constant quantity, and is inaccurate in the sense that its reading is persistently biased with a fixed offset. Conversely, the second sensor generates disperse readings of the same fixed quantity in repeated trials, which of course, are unbiased on average. By exploiting the precision of the first sensor and compensating its inaccuracy using the second one, the data fusion technique of this paper provides a precise and accurate estimate of the measured quantity.

The motivating example of this paper is an application in displacement (or position) measurement that combines two types of optical encoders: incremental and absolute [1]. Both these devices are widely used for measurement of linear and angular positions, albeit with different concepts. Incremental encoders are developed for high precision measurement of relative position with respect to an unspecified initial point. In other words, their highly precise readings are persistently distorted by some unknown but constant offset, rendering them inaccurate. Incremental encoders are used widely in the computer numerical control (CNC) machines. In order to null the measurement offset in these machines, a calibration phase before normal operation is required to reset all moving parts into some known initial position. Yet, any further inaccuracy accumulated during the normal operation mode (often a long time) is left uncompensated. The developments in this paper provide a viable means to enhance the measurement accuracy by exploiting an auxiliary sensor of the absolute type, which essentially measures the absolute position with low precision.

Sensor fusion has been the subject of substantial research efforts [2]–[5] for a broad spectrum of applications [6]–[17], following different estimation approaches [18]–[23]. Most of these approaches rely on detailed stochastic characterization of the measurement noise and the temporal evolution of the measured quantity. Unlike these approaches, the estimator of this paper is based only on the knowledge of certain bounds on the measurement noise and a deterministic dynamic model for the slowly-varying offset of the inaccurate sensor.

The nonlinear estimator in this paper recursively estimates this offset by establishing certain upper and lower bounds on it in terms of the measurement history of both sensors. Then, the midpoint between these bounds is taken as the *midrange estimation* of the measurement offset of the inaccurate sensor. This estimation is utilized then to compensate for this offset, and thereby, exploit the precision of the inaccurate sensor. Evidenced by analytical evaluation and numerical simulation in this paper, the midrange estimator achieves a reasonable performance for its simple structure and easy implementation with minimal prior knowledge of the sensors.

II. Problem Statement

A scalar quantity x_t is measured by a pair of sensors over the discrete time $t = 1, 2, 3, \ldots$. The first sensor is precise but inaccurate with the reading value y_t given by

$$y_t = x_t + \theta_0, \quad t = 1, 2, 3, \ldots, \tag{1}$$

where the measurement offset θ_0 is an unknown constant in the interval $[-\Theta, \Theta]$. The second sensor, which is accurate but imprecise, generates a reading z_t which is a noisy version of x_t expressed as

$$z_t = x_t + w_t, \quad t = 1, 2, 3, \ldots . \tag{2}$$

The measurement noise $\{w_t\}$ is zero-mean in the sense of

$$\lim_{T\to\infty} \frac{1}{T} \sum_{t=1}^{T} w_t = 0,$$

it is bounded within the interval $[-W, W]$, and entirely spans this interval in the sense that

$$\sup_{t\geqslant 1} w_t = -\inf_{t\geqslant 1} w_t = W. \tag{3}$$

The goal in this paper is to develop an estimation law $\mathcal{E}_t(\cdot)$ to map the observation set $(y_1, y_2, \ldots, y_t, z_1, z_2, \ldots, z_t)$ into an estimate of x_t of the form

$$\hat{x}_t = \mathcal{E}_t(y_1, y_2, \ldots, y_t, z_1, z_2, \ldots, z_t), \quad t = 1, 2, 3, \ldots,$$

This work was supported by the National Science Foundation under Grant No. ECCS-1941944.

The author is with the School of Electrical, Computer, and Biomedical Engineering, Southern Illinois University, Carbondale, IL, 62901 USA email: akomaee@siu.edu.

in such a manner that the resulting estimator outperforms the individual readings of the sensors in some reasonable sense. In particular, the estimate $\hat{x}_t$ must be at least as precise as the accurate sensor (with reading z_t) in the sense that

$$|x_t - \hat{x}_t| \leqslant W, \quad t = 1, 2, 3, \ldots. \tag{4}$$

Moreover, it must be asymptotically consistent in the sense

$$\lim_{t \to \infty} |x_t - \hat{x}_t| = 0. \tag{5}$$

In a more practical scenario, the measurement offset of the inaccurate sensor slowly varies with time, i.e., θ_0 in (1) is replaced with θ_t. This offset is assumed bounded within the interval $\theta_t \in [-\Theta, \Theta]$ and evolves in time according to a first order linear dynamics. Then, the reading of the inaccurate sensor is expressed as

$$\theta_t = \alpha \theta_{t-1} + (1 - \alpha)\,\xi_t, \quad t = 1, 2, 3, \ldots \tag{6a}$$

$$y_t = x_t + \theta_t, \tag{6b}$$

where $0 < \alpha < 1$ is a constant, ξ_t, $t = 1, 2, 3, \ldots$ is a noise sequence confined within the interval $\xi_t \in [-\Theta, \Theta]$, and the initial state θ_0 is an unknown in the interval $\theta_0 \in [-\Theta, \Theta]$. To enforce the assumption that y_t is the reading of a precise sensor, the constant ratio

$$\eta = \frac{(1 - \alpha)\,\Theta}{W} \tag{7}$$

must be much smaller than 1 (i.e., $0 < \eta \ll 1$), maintaining that θ_t only slowly varies in time. Moreover, $\Theta \gg W$ reflects the assumption that y_t is inaccurate compared to z_t.

Even though the measurement model (1) is a special case of (6) with $\alpha = 1$, the behavior of its associated estimator fundamentally differs from the more general case of $\alpha \neq 1$. For $\alpha \neq 1$, it is usually impossible to develop an estimator $\hat{x}_t$ to be asymptotically consistent in the sense (5). Hence, the consistency requirement is relaxed into the weaker condition

$$|x_t - \hat{x}_t| \ll W, \quad t \to \infty$$

for $\alpha \neq 1$. Yet, the condition (4) is attainable for $\alpha \neq 1$, and is met by the estimator developed in this paper.

The problem setting in this paper does not include any specific model for the noise sequences $\{\xi_t\}$ and $\{w_t\}$ beyond the bounds $|\xi_t| \leqslant \Theta$ and $|w_t| \leqslant W$, and for the initial state θ_0 beyond $|\theta_0| \leqslant \Theta$. Also, it does not involve any model for the temporal evolution of the measured quantity x_t. Therefore, the estimator design procedure in Section III is based only on the bounds on noise and initial state without any reference to the nature of the measured quantity. Later in Section IV, the estimation performance is evaluated statistically based on stochastic models for $\{\xi_t\}$, $\{w_t\}$, and θ_0.

III. Midrange Estimator

This section proposes a nonlinear estimator in a recursive form in order to address the estimation problem of Section II. The development process for this estimator is similar for both cases of $\alpha = 1$ and $\alpha \neq 1$, while its performance evaluation is presented separately for these cases.

Since a specific model for the measured quantity x_t is not available, this quantity is first removed from the measurement models by subtracting (2) from (6b). Next, (6) is rewritten as the linear state-space model

$$\theta_t = \alpha \theta_{t-1} + (1 - \alpha)\,\xi_t, \quad t = 1, 2, 3, \ldots \tag{8a}$$

$$y_t - z_t = \theta_t - w_t \tag{8b}$$

with the state θ_t, the output $y_t - z_t$, the process noise ξ_t, and the measurement noise $-w_t$. Based on this model, a state estimator is developed next to generate $\hat{\theta}_t$ as an estimate for the measurement offset θ_t. By replacing θ_t in (6b) with $\hat{\theta}_t$, an estimate of x_t is constructed as

$$\hat{x}_t = y_t - \hat{\theta}_t.$$

To generate the estimation $\hat{\theta}_t$, the strategy in this paper is to establish an upper bound U_t and a lower bound L_t on θ_t, and then, take the midpoint

$$\hat{\theta}_t = \frac{L_t + U_t}{2} \tag{9}$$

between these bounds as the estimate $\hat{\theta}_t$ for θ_t. As shown in Proposition 1 below, such upper and lower bounds can be obtained recursively from the nonlinear state-space equations

$$L_t = \max\{\alpha L_{t-1} - (1 - \alpha)\,\Theta, y_t - z_t - W\} \tag{10a}$$

$$U_t = \min\{\alpha U_{t-1} + (1 - \alpha)\,\Theta, y_t - z_t + W\} \tag{10b}$$

for $t = 1, 2, 3, \ldots$, starting from the initial state

$$-L_0 = U_0 = \Theta. \tag{11}$$

Then, in terms of L_t and U_t, the estimate $\hat{x}_t$ of x_t is given by

$$\hat{x}_t = y_t - \frac{L_t + U_t}{2} \tag{12}$$

referred to as midpoint estimator in this paper.

Proposition 1: Suppose that θ_t is generated by (8a) with the initial state $\theta_0 \in [-\Theta, \Theta]$, the process noise $\xi_t \in [-\Theta, \Theta]$, and the measurement noise $w_t \in [-W, W]$. Let $y_t - z_t$ be given by (8b) and assume that L_t and U_t, $t = 1, 2, 3, \ldots$ are generated recursively from the state-space equations (10) with the initial state (11). Then, θ_t is bounded in the interval

$$\theta_t \in [L_t, U_t], \quad t = 1, 2, 3, \ldots. \tag{13}$$

Proof: The proof is straightforward by induction. By taking (11) as the initial state, (13) trivially holds for $t = 0$. Assuming that (13) holds for $t - 1$, the bounds

$$\alpha L_{t-1} - (1 - \alpha)\,\Theta \leqslant \theta_t \leqslant \alpha U_{t-1} + (1 - \alpha)\,\Theta \tag{14}$$

on θ_t are imposed by (8a), while (8b) bounds θ_t within

$$y_t - z_t - W \leqslant \theta_t \leqslant y_t - z_t + W. \tag{15}$$

Then, (13) must hold for t as the intersection of (14) and (15). ■

For the special case of $\alpha = 1$, the recursive equations (10) reduce to

$$L_t = \max\{L_{t-1}, y_t - z_t - W\}$$

$$U_t = \min\{U_{t-1}, y_t - z_t + W\}$$

with the initial state $-L_0 = U_0 = \Theta$. An argument parallel to the proof of Proposition 1 indicates that L_t and U_t bound θ_0 within the interval $\theta_0 \in [L_t, U_t]$, $t = 1, 2, 3, \ldots$.

For the midrange estimator (12), the estimation error

$$\varepsilon_t = x_t - \hat{x}_t$$

is equal to

$$\varepsilon_t = \hat{\theta}_t - \theta_t. \tag{16}$$

This error is clearly bounded within the uncertainty interval

$$\varepsilon_t \in [-r_t, r_t], \quad t = 1, 2, 3, \ldots,$$

where the uncertainty range $r_t \geqslant 0$ is defined as

$$r_t = \frac{U_t - L_t}{2}. \tag{17}$$

Therefore, the bounds L_t and U_t determined from (10), not only provide an estimation for x_t, but also offer a bound on the estimation error, which is dynamically adjusted in time.

The performance of the estimator (12) can be conveniently evaluated in terms of the size and temporal evolution of the uncertainty range r_t. To facilitate the evaluation process, both variables r_t and ε_t are expressed solely in terms of the initial state θ_0 and the noise sequences $\{\xi_t\}$ and $\{w_t\}$ by defining

$$\delta L_t = L_t - \theta_t \leqslant 0, \qquad \delta U_t = U_t - \theta_t \geqslant 0.$$

It is straightforward to conclude from (8) and (10) that δL_t and δU_t evolve in time according to

$$\begin{aligned} \delta L_t &= \max\left\{\alpha \delta L_{t-1} - (1-\alpha)(\xi_t + \Theta), -w_t - W\right\} \\ \delta U_t &= \min\left\{\alpha \delta U_{t-1} - (1-\alpha)(\xi_t - \Theta), -w_t + W\right\} \end{aligned} \tag{18}$$

with the initial state

$$\delta L_0 = -\theta_0 - \Theta, \qquad \delta U_0 = -\theta_0 + \Theta.$$

Then, ε_t and r_t are expressed in terms of δL_t and δU_t as

$$\varepsilon_t = \frac{\delta L_t + \delta U_t}{2} \tag{19}$$

$$r_t = \frac{\delta U_t - \delta L_t}{2}. \tag{20}$$

The following proposition establishes bounds on ε_t and r_t and verifies that the estimator (12) meets its requirement (4).

Proposition 2: Let the assumptions of Proposition 1 hold and define ε_t and r_t according to (16) and (17), respectively. Then, ε_t and r_t are bounded within the intervals

$$\varepsilon_t \in [-W, W], \quad r_t \in [0, W], \quad t = 1, 2, 3, \ldots. \tag{21}$$

Proof: It is concluded from (18) that $\delta L_t \geqslant -w_t - W$ and $\delta U_t \leqslant -w_t + W$. Substituting these inequalities into (20) results in $r_t \leqslant W$, which in turn leads to $r_t \in [0, W]$ as r_t is nonnegative by construction. Using the triangle inequality, it is concluded from (19) that $|\varepsilon_t| \leqslant r_t$, which further results in $|\varepsilon_t| \leqslant W$, or equivalently $\varepsilon_t \in [-W, W]$. ■

For the special case of $\alpha = 1$, typically, the uncertainty in the measurement offset θ_0 is much larger than that of the measurement noise $\{w_t\}$, i.e., $\Theta \gg W$. Therefore, Θ can be effectively taken as $\Theta \to \infty$. In this case, the bounds δL_t and δU_t are independent of θ_0 and are explicitly given by

$$\begin{aligned} \delta L_t &= -\min_{1 \leqslant k \leqslant t} w_k - W \\ \delta U_t &= -\max_{1 \leqslant k \leqslant t} w_k + W. \end{aligned}$$

These explicit expressions, in turn, lead to

$$\varepsilon_t = -\frac{1}{2}\left(\min_{1 \leqslant k \leqslant t} w_k + \max_{1 \leqslant k \leqslant t} w_k\right) \tag{22}$$

$$r_t = W - \frac{1}{2}\left(\max_{1 \leqslant k \leqslant t} w_k - \min_{1 \leqslant k \leqslant t} w_k\right), \tag{23}$$

which simply confirm the same bounds (21) in Proposition 2. Moreover, under the assumption (3) on $\{w_t\}$, they result in

$$\lim_{t \to \infty} \varepsilon_t = 0, \qquad \lim_{t \to \infty} r_t = 0,$$

which clearly verify the consistency condition (5).

IV. Statistical Performance Analysis

This section is dedicated to performance evaluation of the midrange estimator (12) by exploiting stochastic models. Specifically, $\{w_t\}$ and $\{\xi_t\}$ are characterized by statistically independent white sequences uniformly distributed over the intervals $[-W, W]$ and $[-\Theta, \Theta]$, respectively. Also, the initial state θ_0 is represented by a random variable with a uniform distribution on $[-\Theta, \Theta]$ and independent of $\{w_t\}$ and $\{\xi_t\}$. Based on these stochastic models, the performance of (12) is separately analyzed for two cases of $\alpha = 1$ and $0 < \alpha < 1$, corresponding to a constant measurement offset θ_0 and a time-varying θ_t, respectively.

A. Constant Measurement Offset

Under $\alpha = 1$, the estimation error ε_t and the uncertainty range r_t are explicitly given by (22) and (23), respectively. The odd symmetry of ε_t with respect to $w_1, w_2, \ldots, w_t$ as indicated by (22) implies

$$\mathrm{E}[\varepsilon_t] = 0, \quad t = 1, 2, 3, \ldots,$$

which means the estimator (9), and consequently (12), are unbiased. The mean absolute and mean squared estimation errors $\mathrm{E}[|\varepsilon_t|]$ and $\mathrm{E}\left[\varepsilon_t^2\right]$, as well as the mean uncertainty range $\mathrm{E}[r_t]$ are explicitly determined in the next proposition.

Proposition 3: Assume $\{w_t\}$ is a sequence of independent random variables uniformly distributed on $[-W, W]$. Then, for ε_t and r_t given by (22) and (23), it holds that

$$\mathrm{E}[|\varepsilon_t|] = \frac{1}{2}\mathrm{E}[r_t] = \frac{W}{t+1} \tag{24}$$

$$\mathrm{E}\left[\varepsilon_t^2\right] = \frac{2W^2}{(t+1)(t+2)}. \tag{25}$$

Proof: Since the distribution of $m_t \triangleq \max_{1 \leqslant k \leqslant t} w_k$ and $-\min_{1 \leqslant k \leqslant t} w_k$ are the same, (23) implies that

$$\mathrm{E}[r_t] = W - \mathrm{E}[m_t].$$

With some efforts, the probability density function of m_t is obtained as

$$f_{m_t}(z) = \frac{t}{2W}\left(\frac{z+W}{2W}\right)^{t-1}, \quad |z| \leqslant W,$$

which leads to

$$\mathrm{E}[r_t] = W - \int_{-W}^{W} \frac{t}{2W}\left(\frac{z+W}{2W}\right)^{t-1} z dz = \frac{2W}{t+1}.$$

With more efforts, the probability density function of ε_t in (22) can be determined as[1]

$$f_{\varepsilon_t}(z) = \frac{t}{2W}\left(1-\frac{|z|}{W}\right)^{t-1}, \quad |z| \leqslant W.$$

Using this function, the right-hand sides of (24) and (25) are derived from the integrals

$$\mathrm{E}[|\varepsilon_t|] = \int_{-W}^{W} \frac{t}{2W}\left(1-\frac{|z|}{W}\right)^{t-1} |z|\, dz$$
$$\mathrm{E}\left[\varepsilon_t^2\right] = \int_{-W}^{W} \frac{t}{2W}\left(1-\frac{|z|}{W}\right)^{t-1} z^2 dz.$$

■

Proposition 3 indicates that the midrange estimator (12) not only is unbiased, but also is (weakly) consistent (i.e., ε_t tends to 0 in probability as $t \to \infty$). Moreover, the estimation error converges rapidly to 0 with a high rate of $1/t$, which is substantially faster than the convergence rate $1/\sqrt{t}$ of linear estimators. In particular, consider the linear estimator

$$\hat{\vartheta}_t = \frac{1}{t}\sum_{k=1}^{t}(y_k - z_k), \quad t = 1, 2, 3, \ldots$$

that recursively estimates the constant offset θ_0 by averaging the observation sequence $\{y_t - z_t\}$ over time. Even though this estimator is unbiased, its mean squared estimation error slowly converges to 0 according to

$$\mathrm{E}\left[\left(\hat{\vartheta}_t - \theta_t\right)^2\right] = \mathrm{E}\left[\left(\frac{1}{t}\sum_{k=1}^{t} w_t\right)^2\right] = \frac{W^2}{3t},$$

where $\frac{1}{3}W^2$ is the variance of w_t. A comparison between this mean squared error and its counterpart (25) reveals the absolute advantage of the midrange estimator for all $t \geqslant 1$. For instance, at $t = 100$, the midrange estimator achieves the same mean squared error that the linear estimator achieves at $t = 1717$.

B. Time-Varying Measurement Offset

The performance of the midrange estimator (12) for $\alpha \neq 1$ is analyzed in this section using stochastic models. The first result of this section indicates that the midrange estimator is unbiased, i.e., $\mathrm{E}[\varepsilon_t] = 0$. The second main result establishes a convergent upper bound $2W\rho_t$ on $\mathrm{E}[r_t]$ such that

$$\mathrm{E}[|\varepsilon_t|] \leqslant \mathrm{E}[r_t] \leqslant 2W\rho_t, \quad t = 1, 2, 3, \ldots. \tag{26}$$

[1]The proof will be presented in a future publication.

In addition, for η defined in (7), it is shown that

$$\rho_\infty = \lim_{t\to\infty} \rho_t \leqslant \frac{\sqrt{\eta}}{\alpha}, \quad \sqrt{\eta} \leqslant \alpha(1-\eta),$$

which leads to

$$\limsup_{t\to\infty} \mathrm{E}[|\varepsilon_t|] \leqslant \limsup_{t\to\infty} \mathrm{E}[r_t] \leqslant 2W\frac{\sqrt{\eta}}{\alpha} \tag{27}$$

for any η and α holding $\sqrt{\eta} \leqslant \alpha(1-\eta)$. The derivation of these results is presented in the remainder of this section.

To facilitate the derivation process, $\{\xi_t\}$, $\{w_t\}$, and θ_0 are normalized into

$$\xi_t^* = -\frac{(1-\alpha)(\xi_t - \Theta)}{2\eta W}, \quad t = 1, 2, 3, \ldots$$
$$w_t^* = -\frac{w_t - W}{2W}, \quad t = 1, 2, 3, \ldots$$
$$\theta_0^* = -\frac{(1-\alpha)(\theta_0 - \Theta)}{2\eta W}.$$

Clearly, $\{\xi_t^*\}$, $\{w_t^*\}$, and θ_0^* are statistically independent and uniformly distributed on $[0, 1]$. Then, δL_t and δU_t can be expressed as $\delta L_t = 2W\ell_t$ and $\delta U_t = 2Wu_t$, where the normalized variables u_t and ℓ_t are recursively generated by

$$\ell_t = \max\{\alpha\ell_{t-1} + \eta(\xi_t^* - 1), w_t^* - 1\} \tag{28a}$$
$$u_t = \min\{\alpha u_{t-1} + \eta\xi_t^*, w_t^*\} \tag{28b}$$

with the initial state

$$\ell_0 = \eta(1-\alpha)^{-1}(\theta_0^* - 1) \tag{29a}$$
$$u_0 = \eta(1-\alpha)^{-1}\theta_0^*. \tag{29b}$$

Proposition 4: Suppose $\{w_t\}$ in (2) is a white sequence with uniform distribution on $[-W, W]$. Let the initial state θ_0 of (6a) be a random variable and $\{\xi_t\}$ a white sequence, both uniformly distributed on $[-\Theta, \Theta]$ and mutually independent of $\{w_t\}$. Assume that the estimation $\hat{x}_t$ of x_t is generated via the midrange estimator (12) in terms of L_t and U_t recursively constructed by (10), starting from the initial state (11). Then, this estimation is unbiased in the sense that

$$\mathrm{E}[x_t - \hat{x}_t] = \mathrm{E}[\varepsilon_t] = 0, \quad t = 1, 2, 3, \ldots.$$

Moreover, for the uncertainty range r_t in (17) it holds that

$$\mathrm{E}[r_t] = 2W\mathrm{E}[u_t], \quad t = 1, 2, 3, \ldots,$$

where u_t is generated by (28b) with the initial state (29b).

Proof: Multiplying both sides of (28a) and (29a) by -1, it is straightforward to show that

$$(-\ell_t) = \min\{\alpha(-\ell_{t-1}) + \eta(1 - \xi_t^*), 1 - w_t^*\}$$
$$(-\ell_0) = \eta(1-\alpha)^{-1}(1 - \theta_0^*).$$

Comparing these equations with (28b) and (29b) and noting that $1 - w_t^*$, $1 - \xi_t^*$, and $1 - \theta_0^*$ have distributions identical to w_t^*, ξ_t^*, and θ_0^*, it is concluded that $\mathrm{E}[-\ell_t] = \mathrm{E}[u_t]$. This result along with $\delta L_t = 2W\ell_t$, $\delta U_t = 2Wu_t$, (19), and (20) complete the proof. ■

The cornerstone of the analysis in this section is a scalar function $\phi(\cdot)$, which is defined in the following proposition and its relevant properties are presented.

Proposition 5: Let w^* and ξ^* be independent random variables distributed uniformly on $[0,1]$, and define the scalar function $\phi(\cdot):[0,\infty)\to[0,1/2]$ as

$$\phi(u)=\mathrm{E}_{(\xi^*,w^*)}\left[\min\{u+\eta\xi^*,w^*\}\right]. \tag{30}$$

Then, this function is both concave and differentiable, and its derivative holds $0\leqslant\phi'(\cdot)\leqslant 1$.

Proof: Since $\min\{u+\eta\xi^*,w^*\}$ is concave in u for any fixed ξ^* and w^*, its expected value $\phi(u)$ is also concave. The expected value in (30) can be expressed as

$$\begin{aligned}\phi(u)&=\int_0^1 \mathrm{E}_{w^*}\left[\min\{u+\eta\xi,w^*\}\right]d\xi\\&=\frac{1}{\eta}\int_u^{u+\eta}\mathrm{E}_{w^*}\left[\min\{s,w^*\}\right]ds,\end{aligned}$$

which clearly admits the derivative

$$\phi'(u)=\frac{\mathrm{E}_{w^*}\left[\min\{u+\eta,w^*\}\right]-\mathrm{E}_{w^*}\left[\min\{u,w^*\}\right]}{\eta}.$$

This expression is rewritten as

$$\phi'(u)=1+\frac{\mathrm{E}_{w^*}\left[\min\{u,w^*-\eta\}\right]-\mathrm{E}_{w^*}\left[\min\{u,w^*\}\right]}{\eta}$$

to verify $\phi'(\cdot)\leqslant 1$, noting that the second term on the right-hand side is nonpositive. Furthermore, $\phi(\cdot)$ is an increasing function, which verifies $\phi'(\cdot)\geqslant 0$. ■

The next proposition together with Proposition 4 establish the upper bound (26) on the mean absolute estimation error.

Proposition 6: Suppose the deterministic sequence $\{\rho_t\}$ is generated recursively by

$$\rho_t=\phi(\alpha\rho_{t-1}),\quad t=1,2,3,\ldots \tag{31a}$$

$$\rho_0=\tfrac{1}{2}\eta(1-\alpha)^{-1} \tag{31b}$$

in terms of the scalar function $\phi(\cdot)$ in (30). Assume further that the random sequence $\{u_t\}$ is generated by (28b) with the initial state (29b). Then, it holds that

$$\mathrm{E}[u_t]\leqslant\rho_t,\quad t=1,2,3,\ldots. \tag{32}$$

Moreover, the sequence $\rho_1,\rho_2,\rho_3,\ldots$ is convergent to the unique solution to the algebraic equation

$$\rho_\infty=\phi(\alpha\rho_\infty). \tag{33}$$

Proof: Taking the expected value of both sides of (28b) results in

$$\begin{aligned}\mathrm{E}[u_t]&=\mathrm{E}\left[\min\{\alpha u_{t-1}+\eta\xi_t^*,w_t^*\}\right]\\&=\mathrm{E}\big[\mathrm{E}\left[\min\{\alpha u_{t-1}+\eta\xi_t^*,w_t^*\}\,|u_{t-1}\right]\big]\\&=\mathrm{E}\left[\phi(\alpha u_{t-1})\right],\end{aligned}$$

where the second equality is the law of total expectation [24], and the third one is concluded from the definition of $\phi(\cdot)$ in (30) and the fact that (ξ_t^*,w_t^*) and u_{t-1} are mutually independent. As $\phi(\cdot)$ is concave by Proposition 5, Jensen's inequality [24] implies

$$\mathrm{E}[u_t]\leqslant\phi(\alpha\mathrm{E}[u_{t-1}]).$$

This result along with $\mathrm{E}[u_0]=\frac{1}{2}\eta(1-\alpha)^{-1}$ verifies (32).

Since $0\leqslant\phi'(\cdot)\leqslant 1$ holds by Proposition 5, $\phi(\alpha(\cdot))$ is a contraction mapping for $0<\alpha<1$. Therefore, the algebraic equation (33) admits a unique solution, which is the limit of the sequence $\{\rho_t\}$ as $t\to\infty$. ■

Proposition 7 below together with Proposition 4 establish the upper bound (27) on the mean absolute estimation error.

Proposition 7: For any $0<\alpha<1$ and $\sqrt{\eta}\leqslant\alpha(1-\eta)$, the solution ρ_∞ to the algebraic equation (33) holds

$$0\leqslant\rho_\infty\leqslant\frac{\sqrt{\eta}}{\alpha}. \tag{34}$$

Proof: For any $u\leqslant(1-\eta)$ and $0<\eta<1$, the scalar function $\phi(\cdot)$ defined in (30) is explicitly expressed as

$$\phi(u)=\tfrac{1}{2}\eta\left(1-\tfrac{1}{3}\eta\right)+\left(1-\tfrac{1}{2}\eta\right)u-\tfrac{1}{2}u^2.$$

For this expression, the algebraic equation (33) is given by

$$\alpha^2\rho_\infty^2+2\left(1-\alpha+\tfrac{1}{2}\eta\alpha\right)\rho_\infty-\eta\left(1-\tfrac{1}{3}\eta\right)=0,$$

which can be rearranged as

$$\alpha^2\rho_\infty^2-\eta=-2\left(1-\alpha+\tfrac{1}{2}\eta\alpha\right)\rho_\infty-\tfrac{1}{3}\eta^2\leqslant 0.$$

Then, (34) is concluded by solving the inequality

$$\alpha^2\rho_\infty^2-\eta\leqslant 0.$$

Of course, this result holds true if $\rho_\infty\leqslant(1-\eta)$, which is clearly implied by $\sqrt{\eta}\leqslant\alpha(1-\eta)$. ■

C. Simulation Results

The performance of the midrange estimator (12) is further investigated by computer simulations. With the parameter values $1-\alpha=5\times10^{-7}$ and $\eta=0.001$, sample paths of the normalized variables $\varepsilon_t^*=\varepsilon_t/2W$ and $r_t^*=r_t/2W$ were generated in terms of ℓ_t and u_t recursively computed via (28) and (29). For these parameter values, the variance of θ_t is the same as w_t in the steady state. Typical sample paths of $\{\varepsilon_t^*\}$ and $\{r_t^*\}$ are illustrated in Fig. 1 during the initial transient period (top) and in the stationary regime (bottom).

The expected values $\mathrm{E}[|\varepsilon_t^*|]$ and $\mathrm{E}[r_t^*]$ were numerically computed for $t=1,2,\ldots,500$ by averaging over $200,000$ sample paths generated independently. In addition, the upper bound ρ_t was recursively computed from (31) for the same period $t=1,2,\ldots,500$. The results of these computations are illustrated in Fig. 2.

According to this figure, the transient time of the proposed midrange estimator is about $T=100$ samples, which is far shorter than the transient time of the measurement offset θ_t, noting that $\alpha^T\simeq 1-5\times10^{-5}\simeq 1$. It is further observed from Fig. 2 that ρ_t is a relatively tight upper bound of $\mathrm{E}[r_t^*]$, but $\mathrm{E}[r_t^*]$ is not necessarily the same tight bound for $\mathrm{E}[|\varepsilon_t^*|]$. Specifically, in the steady state, ρ_t is only 1.13 times larger than $\mathrm{E}[r_t^*]$, while $\mathrm{E}[r_t^*]$ is 3.34 times larger than $\mathrm{E}[|\varepsilon_t^*|]$.

The numerical results in Fig. 2 predict a steady-state mean absolute error of about $\mathrm{E}[|\varepsilon_t|]=0.008W$ for the midrange estimator (12) versus $\mathrm{E}[|w_t|]=0.5W$, obtained analytically for the "single-measurement" estimator $\hat{x}_t^s=z_t$. Hence, the two-sensor scheme of this paper, equipped with the midrange

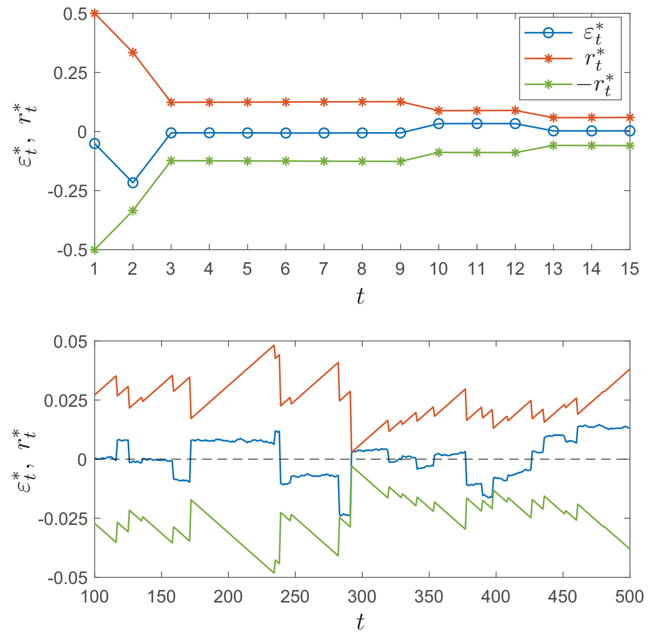

Fig. 1. Typical sample paths of $\{\varepsilon_t^*\}$ and $\{r_t^*\}$: (top) during the initial transient period, and (bottom) in the stationary regime.

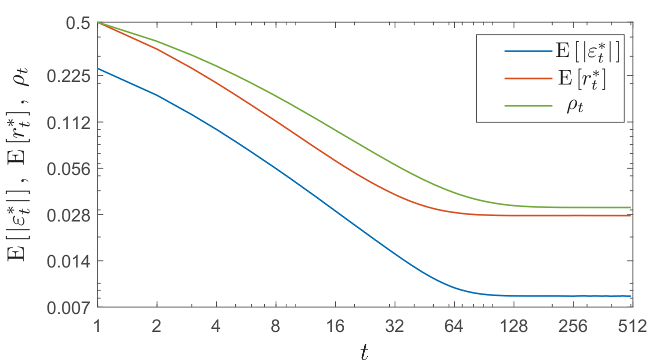

Fig. 2. Normalized mean absolute estimation error $\mathrm{E}\left[|\varepsilon_t^*|\right]$, normalized mean uncertainty range $\mathrm{E}\left[r_t^*\right]$, and the upper bound ρ_t versus time.

estimator (12), improves the accuracy of measurement by a factor of $0.5/0.008 = 62.5$ compared to a single imprecise sensor. Note that for the latter simple measurement scheme, the estimation $\hat{x}_t^s = z_t$ is the only option, since a model for the temporal evolution of the measured quantity x_t does not exist, or it exists but is not informative. A rapidly varying x_t, for instance, might be modeled by a high bandwidth Markov process (or even white process), but dynamic estimation with such a rapidly varying signal can barely improve $\hat{x}_t^s = z_t$.

V. Conclusion

A nonlinear estimator was developed to integrate a pair of sensors, one precise but inaccurate and the other one accurate but imprecise, into a single measurement unit with enhanced precision and accuracy. This estimator has a simple recursive structure, and is implemented based on minimal knowledge of the measurement noise. Despite its simple structure, the proposed estimator was verified effective both analytically and by Monte Carlo simulations.

References

[1] J. Fraden, *Handbook of Modern Sensors: Physics, Designs, and Applications*. New York: Springer, 2010.
[2] J. K. Hackett and M. Shah, "Multi-sensor fusion: A perspective," in *Proc. of IEEE International Conference on Robotics and Automation*, pp. 1324–1330, 1990.
[3] B. V. Dasarathy, "Sensor fusion potential exploitation—innovative architectures and illustrative applications," *Proceedings of the IEEE*, vol. 85, no. 1, pp. 24–38, 1997.
[4] J. Z. Sasiadek, "Sensor fusion," *Annual Reviews in Control*, vol. 26, no. 2, pp. 203–228, 2002.
[5] W. Elmenreich, "A review on system architectures for sensor fusion applications," in *IFIP International Workshop on Software Technolgies for Embedded and Ubiquitous Systems*, pp. 547–559, 2007.
[6] A. Mirabadi, N. Mort, and F. Schmid, "Application of sensor fusion to railway systems," in *Proc. of 1996 IEEE/SICE/RSJ International Conference on Multisensor Fusion and Integration for Intelligent Systems*, pp. 185–192, 1996.
[7] M. Kam, X. Zhu, and P. Kalata, "Sensor fusion for mobile robot navigation," *Proceedings of the IEEE*, vol. 85, no. 1, pp. 108–119, 1997.
[8] J. D. Hol, T. B. Schön, F. Gustafsson, and P. J. Slycke, "Sensor fusion for augmented reality," in *Proc. of 9th International Conference on Information Fusion*, pp. 1–6, 2006.
[9] P. Rybski, P. Anderson-Sprecher, D. Huber, C. Niessl, and R. Simmons, "Sensor fusion for human safety in industrial workcells," in *Proc. of 2012 IEEE/RSJ International Conference on Intelligent Robots and Systems*, pp. 3612–3619, 2012.
[10] H. Cho, Y.-W. Seo, B. V. Kumar, and R. R. Rajkumar, "A multi-sensor fusion system for moving object detection and tracking in urban driving environments," in *Proc. of 2014 IEEE International Conference on Robotics and Automation*, pp. 1836–1843, 2014.
[11] R. O. Chavez-Garcia and O. Aycard, "Multiple sensor fusion and classification for moving object detection and tracking," *IEEE Transactions on Intelligent Transportation Systems*, vol. 17, no. 2, pp. 525–534, 2015.
[12] D. Xu, D. Anguelov, and A. Jain, "PointFusion: Deep sensor fusion for 3D bounding box estimation," in *Proc. of the IEEE Conference on Computer Vision and Pattern Recognition*, pp. 244–253, 2018.
[13] Z. Wang, Y. Wu, and Q. Niu, "Multi-sensor fusion in automated driving: A survey," *IEEE Access*, vol. 8, pp. 2847–2868, 2019.
[14] J. Fayyad, M. A. Jaradat, D. Gruyer, and H. Najjaran, "Deep learning sensor fusion for autonomous vehicle perception and localization: A review," *Sensors*, vol. 20, no. 15, p. 4220, 2020.
[15] M. B. Alatise and G. P. Hancke, "A review on challenges of autonomous mobile robot and sensor fusion methods," *IEEE Access*, vol. 8, pp. 39830–39846, 2020.
[16] D. J. Yeong, G. Velasco-Hernandez, J. Barry, and J. Walsh, "Sensor and sensor fusion technology in autonomous vehicles: A review," *Sensors*, vol. 21, no. 6, p. 2140, 2021.
[17] P. Karle, F. Fent, S. Huch, F. Sauerbeck, and M. Lienkamp, "Multi-modal sensor fusion and object tracking for autonomous racing," *IEEE Transactions on Intelligent Vehicles*, vol. 8, no. 7, pp. 3871–3883, 2023.
[18] H. P. Moravec, "Sensor fusion in certainty grids for mobile robots," *AI Magazine*, vol. 9, no. 2, pp. 61–61, 1988.
[19] R. Olfati-Saber and J. S. Shamma, "Consensus filters for sensor networks and distributed sensor fusion," in *Proc. of the 44th IEEE Conference on Decision and Control (CDC)*, pp. 6698–6703, 2005.
[20] L. Xiao, S. Boyd, and S. Lall, "A scheme for robust distributed sensor fusion based on average consensus," in *Proc. of IPSN 2005. Fourth International Symposium on Information Processing in Sensor Networks*, pp. 63–70, 2005.
[21] N. Ghosh, Y. Ravi, S. Mukhopadhyay, A. Patra, S. Paul, A. Mohanty, A. Chattopadhyay, and A. Chattopadhyay, "Few strategies to improve sensor fusion," in *Proc. of 2006 IEEE International Conference on Industrial Technology*, pp. 1361–1366, 2006.
[22] S. Lynen, M. W. Achtelik, S. Weiss, M. Chli, and R. Siegwart, "A robust and modular multi-sensor fusion approach applied to MAV navigation," in *Proc. of 2013 IEEE/RSJ International Conference on Intelligent Robots and Systems*, pp. 3923–3929, 2013.
[23] W. Yi, G. Li, and G. Battistelli, "Distributed multi-sensor fusion of PHD filters with different sensor fields of view," *IEEE Transactions on Signal Processing*, vol. 68, pp. 5204–5218, 2020.
[24] A. N. Shiryaev, *Probability*. New York: Springer, 2nd ed., 1996.